

Cite this: *RSC Adv.*, 2018, 8, 25361

# Reduced graphene oxide-polyaniline film as enhanced sensing interface for the detection of loop-mediated-isothermal-amplification products by open circuit potential measurement†

Vu Thi Thu,<sup>ab</sup> Bui Quang Tien,<sup>cd</sup> Dau Thi Ngoc Nga,<sup>ab</sup> Ly Cong Thanh,<sup>ce</sup> Le Hoang Sinh,<sup>f</sup> Tu Cam Le<sup>g</sup> and Tran Dai Lam<sup>id</sup>\*<sup>bc</sup>

The development of low cost, portable diagnostic tools for in-field detection of viruses and other pathogenic microorganisms is in great demand but remains challenging. In this study, a novel approach based on reduced graphene oxide-polyaniline (rGO-PANi) film for the *in situ* detection of loop-mediated-isothermal-amplification (LAMP) products by means of open circuit potential measurement is proposed. The pH-sensitive conducting polymer PANi was electro-deposited onto rGO coated screen printed electrodes and tuned to be at the emeraldine state at which the pH sensitivity was maximized. By combining PANi and rGO, the pH sensitivity of the system was modulated up to about  $-64$  mV per pH unit. This enabled the number of amplified amplicons resulting from the isothermal amplification process to be monitored. The sensor was then examined for monitoring LAMP reactions using Hepatitis B virus (HBV) as a model. This simple, low-cost, reproducible and sensitive interfacing layer is expected to provide a new possibility for designing point-of-care sensors under limited-resource conditions.

Received 12th May 2018  
Accepted 11th July 2018

DOI: 10.1039/c8ra04050h

rsc.li/rsc-advances

## Introduction

There is currently a great need for developing portable diagnostic tools for in-field detection of viruses and other pathogenic microorganisms in resource-limited settings. These platforms offer many advantages for detection of various pathogens including portability, automation, speed, cost, and efficiency.<sup>1</sup> In order to achieve highly sensitive and early target detection, the molecular amplification technologies should be integrated onto such diagnostic tools. Loop-mediated isothermal amplification (LAMP) is one of the most advanced genetic techniques that can provide extremely fast sequential progression (less than 1 hour)<sup>2</sup> and relatively high selectivity (100-fold greater than conventional PCR<sup>3</sup>). Using this

technique, the gene amplification is performed under isothermal conditions within a short diagnostic time using six gene regions, and only one type of enzyme (Bst polymerase).<sup>4,5</sup> To monitor the amplification process in LAMP reactions, optical aids such as turbidity, fluorescence, and pH sensitive dyes, using which the by-product of LAMP reactions (magnesium pyrophosphate) can be recorded, are employed to determine the amplification degree.<sup>6,7</sup> Several works have also reported the use of the electrochemiluminescence technique for quantification of LAMP products.<sup>8,9</sup> Nevertheless, the use of such optical detectors seems to be not suitable to comply with requirements of in-field diagnostic microchips such as low-cost, flexibility, portability and integration ability.

During the last decade, a number of LAMP-based microchips with electrochemical analysis of amplicons has been reported. Several works described the electrochemical record of the LAMP reaction process by monitoring the intercalation of DNA-binding redox reporter molecules (*i.e.*, methylene blue<sup>10</sup>) into newly formed amplicons. Other research groups have demonstrated the voltammetric detection of the amount of deoxy-nucleotide triphosphates (dNTPs) consumed during reaction.<sup>11</sup> Recently, the pH decrease caused by pyrophosphated protons released during LAMP reaction has also been utilized as an indicator for electrochemical analysis of amplicons. For instance, Gosselin *et al.* has developed potentiometric sensor based on polyaniline film to continuously monitor the pH of the solution during the LAMP amplification.<sup>12</sup> The linear

<sup>a</sup>University of Science and Technology of Hanoi (USTH), Vietnam Academy of Science and Technology (VAST), 18 Hoang Quoc Viet, Cau Giay, Hanoi, Vietnam

<sup>b</sup>Center for High Technology Development (HTD), Vietnam Academy of Science and Technology (VAST), 18 Hoang Quoc Viet, Cau Giay, Hanoi, Vietnam. E-mail: trandailam@gmail.com

<sup>c</sup>Graduate University of Science and Technology (GUST), Vietnam Academy of Science and Technology (VAST), 18 Hoang Quoc Viet, Cau Giay, Hanoi, Vietnam

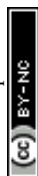
<sup>d</sup>Military Academy of Logistics, Ngoc Thuy, Long Bien, Hanoi, Vietnam

<sup>e</sup>Hanoi University of Pharmacy, 15-17 Le Thanh Tong, Hoan Kiem, Hanoi, Vietnam

<sup>f</sup>Duy Tan University, 03 Quang Trung, Da Nang, Vietnam

<sup>g</sup>School of Engineering, RMIT University, GPO Box 2476, Melbourne, VIC 3001, Australia

† Electronic supplementary information (ESI) available. See DOI: 10.1039/c8ra04050h



calibration of the potentiometric pH measurement, with a slope of  $-83$  mV per pH unit was reported. In previously reported electrochemical detection methods, the output signals are strongly affected by the precipitation of by-products during LAMP reactions. In some cases, different redox molecules must be put in the reaction solution. This can lead to certain side-effects which inhibit sequential process. Therefore, monitoring the number of amplicons using pH change during LAMP reactions is more advantageous.

To sense the pH of the reaction solution, a pH-sensitive thin film should be used. In the case of electrochemical sensing of pH, this thin film must satisfy two critical requirements: high sensitivity to  $H^+$  or  $OH^-$  ions; and high conductivity. The pH-sensitive conducting polymer (*i.e.* polyaniline) meet these criteria.<sup>12,13</sup> In the literature, it is well-known that polyaniline is a pH-sensitive film with the response of about several tens millivolts per pH unit at room temperature. The pH sensitivity of polyaniline is due to the proton doping (protonation) and dedoping (deprotonation) of the conducting oxidative state, namely emeraldine. It was reported that polyaniline has the highest potentiometric response to pH variation compared to other conducting polymers.<sup>14</sup> Our research group has demonstrated the use of polyaniline films to monitor ion concentrations in different sensing configurations and as a pH-sensitive matrix for immobilizing enzymes.<sup>15</sup> Lalit Kumar *et al.* deposited polyaniline films on flexible substrates for ammonia gas sensor<sup>16</sup> while a high-performance flexible pH sensor based on polyaniline nanopillar array defined by soft lithography was reported by Yoon *et al.*<sup>17</sup> However, polyaniline is more conductive at pH less than 5.0 and become less conductive at higher pH range.

To improve the conductivity of polyaniline film at pH range of LAMP reactions (7.0–9.0), carbonaceous materials are top candidates. With their specific electronic structures, graphene and its derivatives offer a superior conductivity and mechanical flexibility that are often required for disposable electrochemical sensing systems. In addition, these materials are biocompatible. A potentiometric pH sensor based on carbon-polyaniline composite was recently developed using direct laser writing for wearable point-of-care applications.<sup>18</sup> Compared to graphene, reduced graphene oxide has similar behaviors including high conductivity, large surface area, and easy functionalization. They can be easily produced *via* chemical routes with low-cost and high yield.<sup>19</sup> The reduced form of graphene oxide (rGO) also has abundant oxygen moieties and can improve the pH sensitivity of polyaniline film.<sup>20</sup> A pH sensor based on polyaniline functionalized by reduced graphene oxide (PANi-rGO) for monitoring microbial fermentation process has been reported.<sup>21</sup> PANi-rGO composite was also shown to have high electrical conductivity and capacitance for efficient electrochemical supercapacitors.<sup>22</sup>

In this work, we demonstrate the use of the highly-sensitive PANi and highly-conductive rGO films to fabricate the device for monitoring pH changes during genetic amplification in LAMP reactions. The film was first fabricated through electrochemical reduction of drop-casted graphene oxide, and

followed by electro-deposition of PANi in acidic solution. The Open Circuit Potential (OCP) measurements were utilized for end-point detection of number of amplified amplicons. It should be emphasized that the measurement of the OCP is highly sensitive and reproducible. Indeed, although such a detection of LAMP products has been shown previously with potentiometric measurement,<sup>12</sup> however, this method could trigger significant oxidation state change of PANi during current/potential imposition measurement, leading to inaccurate signals. By contrast, our OCP technique should provide a simpler and more accurate detection procedure since it can be done without any application of neither potential nor current to the system. Thus, subsequent and multiple measurements could be assured and unambiguously interpreted, without film damage.

## Experimental

### Chemicals

Graphene oxide (GO) was prepared from graphite powder using a modified version of the Hummer's method. Aniline ( $C_6H_5NH_2$ ) was purchased from Sigma Aldrich (USA). Phosphate buffered saline (PBS, pH 7.4) buffer was employed as the supporting electrolyte. All chemicals were of analytical grade and used without further purification, and redistilled water was used throughout. Screen printed carbon electrodes (SPE) with a three-electrode setup (diameter of working electrode is 3 mm) were purchased from Quasense (Thailand). LAMP amplification reagent (Loopamp DNA amplification kit) was provided by Eiken (Japan).

A set of six primers was designed according to literature to specifically target HBV in human blood. The primer set consisted of two outer primers (F3, B3), two inner primers (FIP, BIP), and two loop primers (LF, LB).<sup>23</sup> All primers were commercially synthesized by Macrogen (Seoul, Korea).

### Preparation of rGO/PANi films

The pH-sensitive sensor based on rGO-PANi was prepared on SPE electrode. Firstly, the graphene oxide ( $1\text{ mg ml}^{-1}$ ) was drop-casted onto the electrode. After that, the film was electrochemically reduced by cyclic voltammetry method with potential ranging from 0 V to  $-1.2$  V for several cycles. Finally, polyaniline was electro-deposited by sweeping SPE||rGO electrode in 0.5 M  $H_2SO_4$  solution containing 0.3 M aniline for 10 cycles from  $-200$  mV to  $+900$  mV.

The surface morphology of the electrodes was characterized using a Hitachi S-4800 field emission scanning electron microscopy (FE-SEM) at acceleration voltage of 5 kV. Attenuated total reflectance Fourier transform Infrared Spectra (ATR-FTIR) of the samples were examined using IR-Tracer 100 (Shimadzu, Japan) and the samples were scanned between 500 and  $4000\text{ cm}^{-1}$ . The crystallinity of the prepared samples were determined by Raman spectroscopy in the spectral range  $300\text{--}3500\text{ cm}^{-1}$  using 532 nm excitation source on a Horiba spectrometer.



## pH test

The pH calibration measurements were conducted using PBS buffers with adjusted pH of 6.0–9.0. These buffers were used to measure the open circuit voltage (OCP) variation of the working electrode vs. Ag/AgCl reference electrode due to the pH change. All experiments were conducted at room temperature. All measurements were conducted on a PC-controlled Metrohm Autolab PGSTAT 302N electrochemical workstation (Metrohm Co., Ltd., Switzerland).

## LAMP reaction

The LAMP mixture was prepared as described in our previous work.<sup>23</sup> The phage DNA was diluted with PBS buffer (pH 7.4) to the concentration of  $10 \text{ ng } \mu\text{l}^{-1}$ . A reaction mixture (25  $\mu\text{l}$ ) is consisted of 1.6  $\mu\text{M}$  of the FIP and BIP primers, 0.8  $\mu\text{M}$  of each outer primer (F3 primer and B3 primer), 0.8  $\mu\text{M}$  of each loop primer (LPF primer and LPB primer), reaction mix (12.5  $\mu\text{l}$ ), Bst DNA polymerase (1  $\mu\text{l}$ ), and 5  $\mu\text{l}$  sample. The LAMP reaction was conducted at 65 °C and then stopped at 84 °C after several intervals of time (0, 10, 20, 30, 40, 60 min). The number of amplified amplicons was recorded using OCP measurements in which no current occurred in the electrochemical cell. The LAMP products were also analyzed qualitatively by gel-electrophoresis technique in a 2% agarose gel. The exact concentration of DNA at every reaction step was determined using Nanodrop after the purification of DNA solution.

## Results and discussion

### Preparation of rGO-PANi film

Electro-deposition provides an efficient and versatile route for the synthesis of nanostructured polymers and their composites.<sup>24</sup> In this work, the rGO-PANi film was prepared by the electro-polymerization of aniline (0.3 M) in 0.5 M  $\text{H}_2\text{SO}_4$  solution on the surface of the rGO modified SPE. As seen from Fig. 1(a) which shows reduction of drop-casted graphene oxide material, an intense reduction peak is present at around  $-1000 \text{ mV}$  with the onset potential of  $-900 \text{ mV}$  during the 1<sup>st</sup> cycle of cyclic voltammetry of graphene oxide. In the subsequent cycles, the intensity of the reduction peak decreases dramatically (Fig. 1S†). Meanwhile, there are no anodic peaks for all cycles. This demonstrates the irreversible transition in which graphene oxide was converted completely into its reduced form.<sup>21</sup> The cyclic voltammograms recorded during the electrodeposition of PANi onto rGO film is shown in Fig. 1(b). The continuous increase of current density has indicated the growth of PANi over the rGO surface.<sup>24</sup> The transition between different oxidation states of polyaniline was also observed during deposition process (more details in Fig. 2S†). As seen on cyclic voltammograms in Fig. 1b, the first anodic wave situated at  $+225 \text{ mV}$  (vs. Ag/AgCl) indicates transition of leucoemeraldine form of polyaniline to emeraldine salt while the second anodic wave occurred at  $+565 \text{ mV}$  (vs. Ag/AgCl) denotes formation of fully doped pernigraniline salt.<sup>20</sup> The final scan was stopped at 0 V to obtain emeraldine – the only conductive form of polyaniline.<sup>14,16</sup>

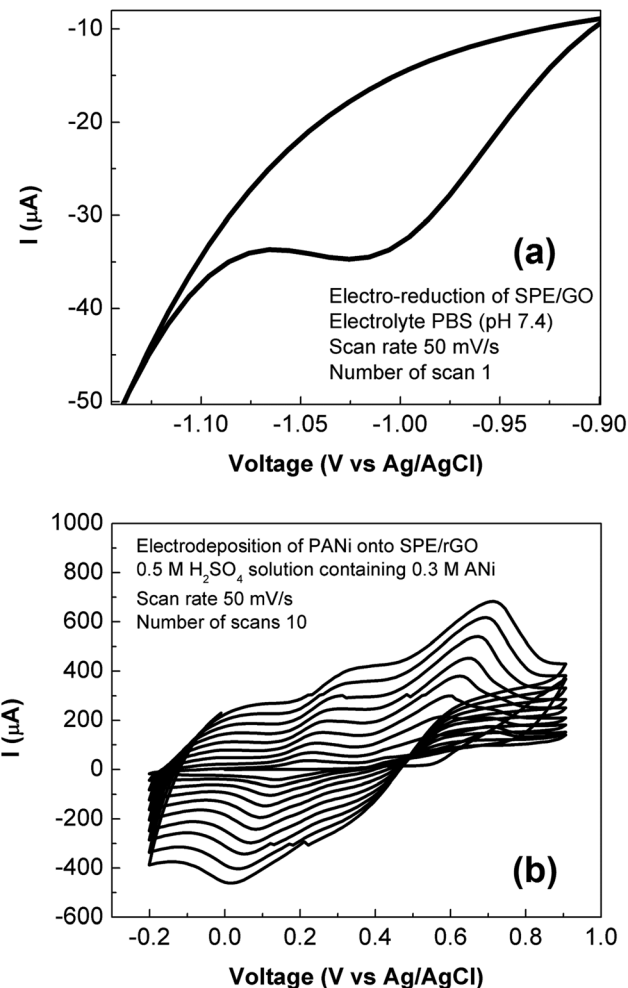


Fig. 1 Preparation of rGO-PANi film. (a) Electro-reduction of graphene oxide coated SPE: the drop-casted graphene oxide film was electrochemically reduced by sweeping in PBS solution (pH 7.4) at scan rate of  $50 \text{ mV s}^{-1}$  for several scans. (b) Electro-deposition of polyaniline onto SPE/rGO: the SPE/rGO electrode film was electrochemically modified by sweeping in 0.5 M  $\text{H}_2\text{SO}_4$  solution containing 0.3 M aniline at scan rate of  $50 \text{ mV s}^{-1}$  for ten scans.

### Structure and morphology of rGO-PANi film

Surface morphology of the rGO film and rGO-PANi film were characterized by FE-SEM (Fig. 2). As can be seen from Fig. 2(a), the rGO 'wrinkles' are present with random distribution on the electrode surface. Meanwhile, the polyaniline film was found to be in a microporous interconnected network (Fig. 2(b)) which is beneficial for electron transport at the electrolyte–electrode interface.<sup>25,26</sup> The size of micropores was in the range of 0.3–0.9  $\mu\text{m}$ . The very thin graphitic layer was completely hidden by the relatively uniform and thick polymeric film ( $\sim 110 \text{ nm}$ ) and cannot be seen by electron microscopy. Therefore, ATR-FTIR and Raman techniques were used to confirm the formation of rGO-PANi film and provide deeper insights on the structure of the composite material.

The ATR-FTIR spectrum of rGO (Fig. 3) reveals the presence of  $\text{C}=\text{C}$  stretching ( $1400\text{--}1600 \text{ cm}^{-1}$ ) and the disappearance of



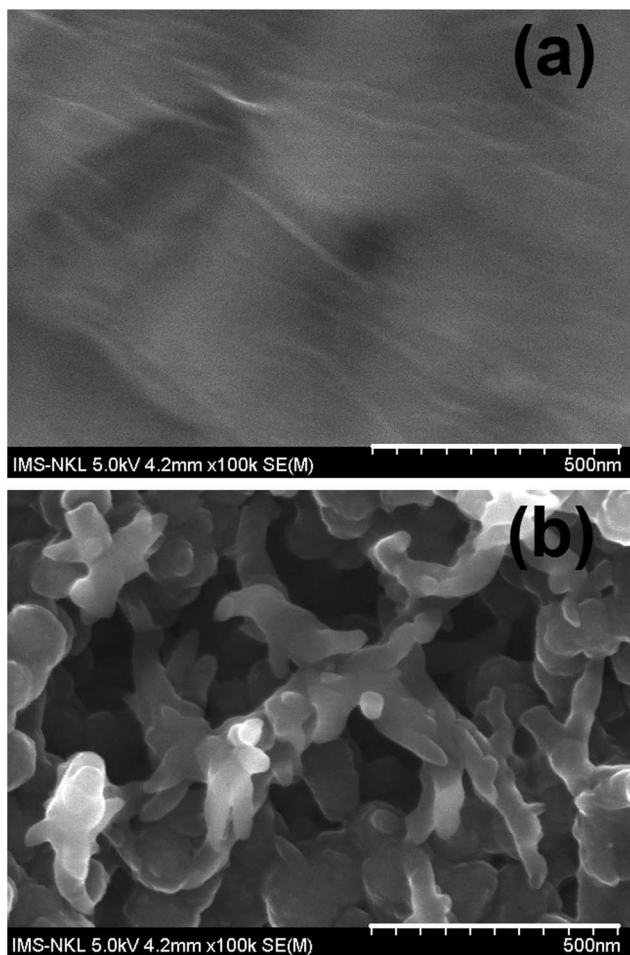


Fig. 2 SEM images of rGO (a) and rGO-PANi (b) films. The polyaniline film was found to be in a microporous interconnected network with the size of micropores was in the range of 0.3–0.9  $\mu\text{m}$ . The very thin graphitic layer was completely hidden by the relatively uniform and thick polymeric film ( $\sim 110$  nm) and cannot be seen by electron microscopy.

$\text{C}=\text{O}$  ( $\sim 1700$   $\text{cm}^{-1}$ ) and  $\text{C}-\text{O}$  ( $\sim 1010$   $\text{cm}^{-1}$ ) stretching of the carboxylic and epoxide group. This result indicates that most of oxygen containing groups on the drop-casted graphene oxide material were eliminated. At the same time, the characteristic bands of the emeraldine structure were clearly obtained on rGO/PANi film after electrodepositing process (Fig. 3): 1564 and 1491  $\text{cm}^{-1}$  ( $\text{C}=\text{C}$  stretch), 1298  $\text{cm}^{-1}$  ( $\text{C}-\text{N}$  stretch), 1134  $\text{cm}^{-1}$  ( $\text{C}=\text{N}$ ), 797  $\text{cm}^{-1}$  ( $\text{C}-\text{H}$ ).<sup>16</sup>

Fig. 4 exhibits Raman spectra of rGO and rGO-PANi films. The peaks at 1335  $\text{cm}^{-1}$ , 1581  $\text{cm}^{-1}$ , 2686  $\text{cm}^{-1}$  are ascribed to typical D, G, and 2D Raman bands of graphitic material, respectively.<sup>27</sup> The D band is related to the defects, edges and structural disorders of solid carbon whilst the G band is associated with the first-order scattering of  $E_{2g}$  mode of  $sp^2$  hybridized carbon. The intensity ratio  $I_D/I_G$  is an effective indicator of the transition between GO and rGO. Here, the Raman spectrum (Fig. 4(a)) of rGO after electrochemical reduction shows a  $I_D/I_G$  ratio of 0.946, significantly higher than that value for GO of 0.803. This indicates that there is an

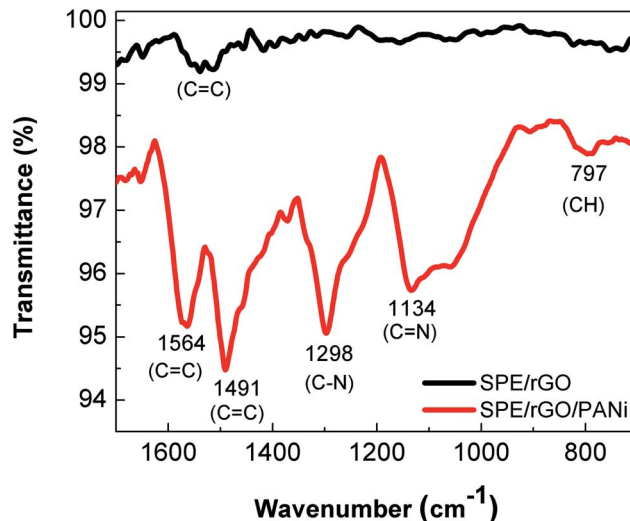


Fig. 3 ATR-FTIR spectra of rGO (black) and rGO-PANi (red) films. For rGO: 1400–1600  $\text{cm}^{-1}$  ( $\text{C}=\text{C}$  stretching), 1010  $\text{cm}^{-1}$  ( $\text{C}-\text{O}$ ). For rGO/PANi: 1564 and 1491  $\text{cm}^{-1}$  ( $\text{C}=\text{C}$  stretch), 1298  $\text{cm}^{-1}$  ( $\text{C}-\text{N}$  stretch), 1134  $\text{cm}^{-1}$  ( $\text{C}=\text{N}$ ), 797  $\text{cm}^{-1}$  ( $\text{C}-\text{H}$ ).

increase in the number of defect sites caused by the removal of the functional groups from GO,<sup>21</sup> and the GO material was electrochemically reduced into rGO. When there is polyaniline electrodeposited on rGO, the positions of the above peaks (Fig. 4(b)) are slightly shifted to longer wavenumbers of 1337  $\text{cm}^{-1}$ , 1585  $\text{cm}^{-1}$  and 2760  $\text{cm}^{-1}$ . The other Raman peaks located at 812, 1164, 1244, 1403, 1483  $\text{cm}^{-1}$  are consistent with amine deformation (benzoid),  $\text{C}-\text{H}$  in-plane bending (benzoid),  $\text{C}-\text{N}^+$  protonated amine stretching (quinoid),  $\text{C}-\text{C}$  stretching (quinoid), and  $\text{N}-\text{H}$  bending (quinoid), respectively (Fig. 4(b)).<sup>24</sup>

#### pH test

The pH response for rGO/PANi film was tested by measuring the OCP potentials at different pH values (6.0–9.0) as depicted in Fig. 5(a). It was found that the OCP value decreased with increasing pH. Two linear regions were obtained at pH ranging from 6.0 to 7.5 and pH ranging from 7.5 to 9.0 with the following regression equations:

$$\text{OCP} = 389.8803 - 64.1524 \times \text{pH} \quad (R^2 = 0.9831) \quad (\text{pH} = 6.0-7.5)$$

$$\text{OCP} = 78.8339 - 23.1149 \times \text{pH} \quad (R^2 = 0.9598) \quad (\text{pH} = 7.5-9.0)$$

The voltage drift caused by pH change of rGO-PANi film is of  $-64$  mV per pH unit which is comparable to those obtained from other polyaniline-based sensors in previously reported works.<sup>12,18,19</sup> Depending on the fabrication process of the electrodes, the slope of the calibration curves ranges from  $-55$  to  $-90$  mV per pH unit. Compared to pristine polyaniline film (Fig. 4S<sup>†</sup>), the composite rGO-PANi exhibits a steeper slope of OCP-pH response curve, probably resulting from high conductivity of rGO material. Indeed, the electron transfer was found to be faster when rGO was deposited on the electrode (Fig. 5S<sup>†</sup>).



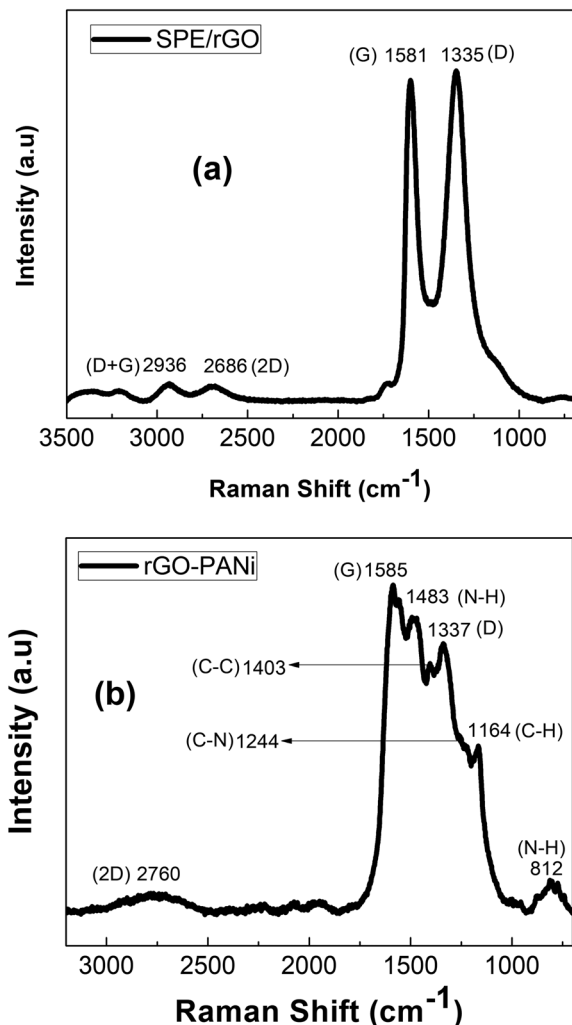


Fig. 4 Raman spectra rGO (a) and rGO-PANI (b) films.

Further improvement in the slope of potential–pH curve can be performed with the use of derivatives of polyaniline.<sup>20</sup>

The pH response mechanism of polyaniline-based sensors depends on the transition from the emeraldine salt to the emeraldine base as documented in the literature.<sup>14</sup> It is generally agreed that PANi exists in three different base forms: leucoemeraldine (colorless, fully reduced, poor conducting),

emeraldine (green, half-oxidized, conducting), and pernigraniline (dark, fully oxidized, poor conducting).<sup>20</sup> The only electrically conducting form is the emeraldine which can suffer from reversible protonation process (Fig. 5(b)) and is therefore sensitive to the acidic/alkalic degree of the solution.<sup>28</sup> This is also the reason why we stopped the electro-deposition of polyaniline film at 0 mV. As the pH increases, the ions in the top-layers of the polymer chains will be transferred to the electrolyte solution during deprotonation process (dedoping). In contrast, the anions in the electrolyte solution can act as charge compensating ions in the protonation process (doping) as the pH decreases. Consequently, the OCP will decrease with increasing pH and *vice versa*. This behavior was also found in other polymers but the highest potentiometric response was reported for polyaniline.<sup>16</sup>

Notably, the protonation and deprotonation processes in polyaniline are reversible.<sup>16</sup> It means that one can easily tune the transition between the emeraldine salt and the emeraldine base by shifting the pH of the solution. On the other hand, this p-type conducting polymer with dual pH sensitivity is sensitive with both negative and positive ions. Thus, our sensor should be reusable in principle. Indeed, we tried to transform emeraldine salt into emeraldine base by sweeping the used electrodes (previously incubated in alkaline electrolytes) in acidic solution without monomer. The experimental results have demonstrated the successful reform of emeraldine base but with a hysteresis (Fig. 6S<sup>†</sup>).

#### LAMP reaction

The detection of LAMP products was conducted on rGO-PANI interface, by means of OCP measurement. The detection mechanism relies on the pH decrease caused by hydronium ions released during the elongation of DNA in LAMP reaction. Fig. 6(a) shows the normalized variation of the measured potential associated with positive and negative LAMP reactions. It was demonstrated that the OCP value increases with reaction time (27 mV over 40 minutes), indicating the increase in the number of amplicons and released protons. Meanwhile, an ignorable decrease in OCP values was found for negative sample (Fig. 6(a)). This demonstrates the high specificity of the sensor.

These results are in good agreement with gel-electrophoresis and absorbance measurements. In Fig. 6(b), positive LAMP

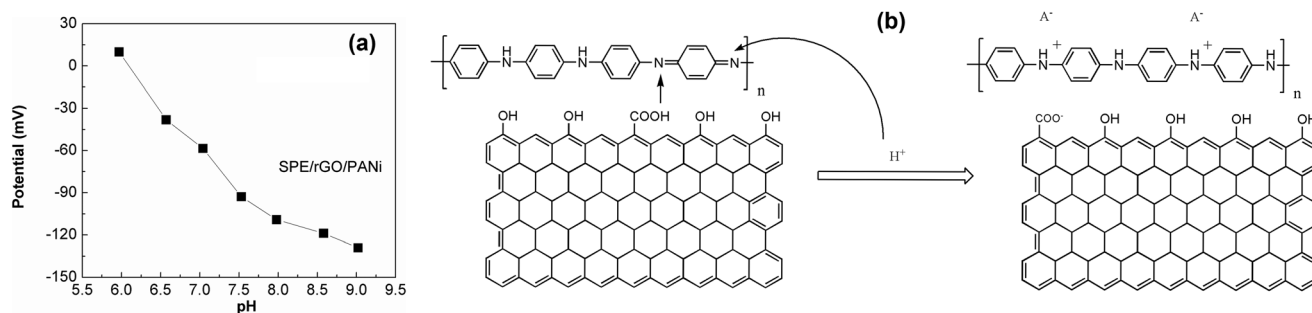


Fig. 5 (a) pH calibration curve of SPE/rGO-PANI electrode. The equilibrium potential increases with decreasing pH due to the protonation of emeraldine base form of polyaniline. pH range 6.0–9.0 (buffered PBS solution). (b) Schematic diagram demonstrating the pH-sensitive mechanism of SPE/rGO-PANI electrode.



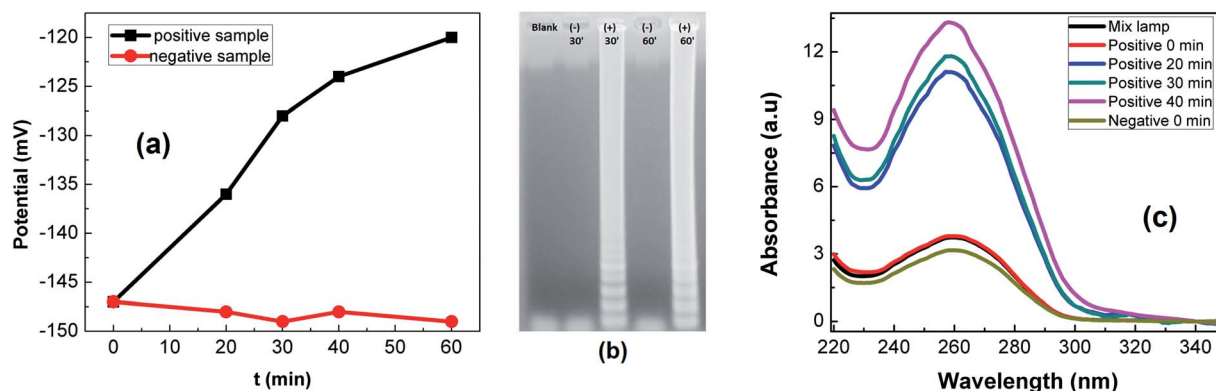


Fig. 6 LAMP reactions: OCP detection (a), gel-electrophoresis (b) and absorbance measurements (c) of LAMP products.

sample shows multiple bands of different sizes upon agarose gel electrophoresis. This is caused by inverted-repeat structures of LAMP products. At the same time, the DNA concentration was found to be increased about  $10^3$ -fold (as determined from absorbance spectra (Fig. 6(c))).

## Conclusions

The pH sensitivity of the rGO-PANI interface was investigated and successfully applied for the detection of LAMP reactions by means of OCP measurement. The rGO ad-layer with high conductivity and intrinsic pH sensitivity has contributed to the overall enhanced sensitivity of the sensing interface. A reduction in OCP value of 27 mV was found for  $10^2$ -times genetic amplification. The incorporation of a microfluidic flow system and microarray configuration will be carried out in further works for simultaneous detection of multiplex pathogens in point-of-care devices.

## Conflicts of interest

There are no conflicts to declare.

## Acknowledgements

This work acknowledges financial support from National Foundation of Science and Technology Development project, code: NAFOSTED 104.04-2014.36 (T.D.L).

## References

- M. Zarei, *Biosens. Bioelectron.*, 2018, **106**, 193.
- T. Notomi, H. Oayama, H. Masubuchi, T. Yonekawa, K. Wanatabe, N. Amoni and T. Hase, *Nucleic Acids Res.*, 2000, **28**, 63e.
- Q. D. Zhang, G. March, V. Noel, B. Piro, S. Reisberg, L. D. Tran, L. V. Hai, E. Abadia, P. E. Nielsen, C. Sola and M. C. Pham, *Biosens. Bioelectron.*, 2012, **32**, 163.
- T. Notomi, Y. Mori, N. Tomita and H. Kanda, *J. Microbiol.*, 2015, **53**, 1.
- M. Safavied, M. K. Kanakasapathy, F. Tarlan, M. U. Admed, M. Zourob, W. Asghar and H. Shafiee, *ACS Biomater. Sci. Eng.*, 2016, **2**, 278.
- N. Tomita, Y. Mori, H. Kanda and T. Notomi, *Nat. Protoc.*, 2008, **3**, 877.
- T. Yoshikawa, T. Matsuo, Y. Kawamura, M. Ohashi, T. Yonekawa, H. Kanda, T. Notomi and M. Ihira, *J. Virol. Methods*, 2014, **201**, 65.
- S. Roy, S. X. Wei, J. L. Z. Ying, M. Safavied and M. U. Admed, *Biosens. Bioelectron.*, 2016, **86**, 346.
- N. F. N. Azam, S. Roy, S. A. Lim and M. U. Admed, *Food Chem.*, 2018, **248**, 29.
- K. Hsieh, A. S. Patterson, B. S. Ferguson, K. W. Plaxco and H. T. Soh, *Angew. Chem., Int. Ed.*, 2012, **124**, 4980.
- K. Qu, Q. Li, Z. Cui, J. Zhao and X. Sun, *Electroanalysis*, 2011, **23**, 2438.
- D. Gosselin, M. Gougis, M. Baque, M. N. Belgacem, D. Chaussy, A. G. Bourdat, P. Mailey and J. Berthier, *Anal. Chem.*, 2017, **89**, 10124.
- C. O. Baker, X. Huang, W. Nelson and R. B. B. Kaner, *Chem. Soc. Rev.*, 2017, **46**, 1510.
- A. A. Karyakin, O. A. Bobrova, L. V. Lukachova and E. E. Karyakina, *Sens. Actuators, B*, 1996, **33**, 34.
- T. T. Cao, H. B. Nguyen, V. T. Nguyen, T. T. Vu, B. Maxime, P. Mattieu, L. S. Jean, B. T. Phan, D. L. Tran, N. M. Phan and V. C. Nguyen, *Sens. Actuators, B*, 2018, **260**, 78.
- L. Kumar, I. Rawal, A. Kaur and S. Annapoorni, *Sens. Actuators, B*, 2017, **240**, 408.
- J. H. Yoon, S. B. Hong, S. O. Yun, S. J. Lee, T. J. Lee, K. G. Lee and B. G. Choi, *J. Colloid Interface Sci.*, 2017, **490**, 53.
- R. Rahim, O. Manuel, T. Ali, K. Shahla, K. Ali and Z. Babak, *ACS Appl. Mater. Interfaces*, 2017, **9**, 9015.
- A. A. Ambrosi, K. C. Chun, N. M. Latiff, A. H. Loo, C. H. A. Wong, A. Y. S. Eng, A. Bonanni and Ma. Pumera, *Chem. Soc. Rev.*, 2016, **45**, 2458.
- T. Lindfors and A. Ivaska, *J. Electroanal. Chem.*, 2002, **531**, 43.
- S. Chinnathambi and G. J. W. Euverink, *Sens. Actuators, B*, 2018, **264**, 38.
- N. A. Kumar, H. J. Choi, Y. R. Shin, D. W. Chang, L. Dai and J. B. Baek, *ACS Nano*, 2012, **6**, 1715.



- 23 Q. T. Bui, T. N. Nguyen, T. L. Nguyen, T. T. Vu and D. L. Tran, *J. Electron. Mater.*, 2017, **46**, 3565.
- 24 R. Sha, K. Komori and S. Badhulika, *Electrochim. Acta*, 2017, **233**, 44.
- 25 X. Mengli, S. Yonghai, Y. Yihan, G. Coucong, S. Yuan, W. Linyu and W. Li, *Sens. Actuators, B*, 2017, **252**, 1187.
- 26 S. Liang, W. Xiaoying, Y. Baiqin, W. Qian, T. Qianqian, J. Zhanyou and Z. Jing, *Electrochim. Acta*, 2017, **255**, 286.
- 27 A. C. Ferrari, J. C. Meyer, V. Scardaci, C. Casiraghi, M. Lazzeri, F. Mauri, S. Piscanec, D. Jiang, K. S. Novoselov, S. Roth and A. K. Geim, *Phys. Rev. Lett.*, 2006, **97**, 187401.
- 28 A. Lewenstam, J. Bobacka and A. Ivaska, *J. Electroanal. Chem.*, 1994, **368**, 23.

